Microcirculation WILEY

Integrated pancreatic microcirculatory profiles of streptozotocin-induced and insulin-administrated type 1 diabetes mellitus

Yuan Li[1] | Bingwei Li[1] | Bing Wang[1] | Mingming Liu[1,2] | Xiaoyan Zhang[1] | Ailing Li[1] | Jian Zhang[1,2] | Honggang Zhang[1] | Ruijuan Xiu[1]

[1]Institute of Microcirculation, Key Laboratory of Microcirculation, Ministry of Health, Chinese Academy of Medical Sciences & Peking Union Medical College, Beijing, China

[2]Diabetes Research Center, Chinese Academy of Medical Sciences & Peking Union Medical College, Beijing, China

Correspondence
Mingming Liu, Honggang Zhang, Institute of Microcirculation, Chinese Academy of Medical Sciences & Peking Union Medical College (CAMS & PUMC), No.5 Dong Dan San Tiao, Dongcheng District, Beijing, 100005, China.
Emails: mingmingliu@imc.pumc.edu.cn; zhanghg1966126@163.com

Abstract

Objective: As an integrated system, pancreatic microcirculatory disturbance plays a vital role in the pathogenesis of type 1 diabetes mellitus (T1DM), which involves changes in microcirculatory oxygen and microhemodynamics. Therefore, we aimed to release type 1 diabetic and insulin-administrated microcirculatory profiles of the pancreas.

Methods: BALB/c mice were assigned to control, T1DM, and insulin-administrated groups randomly. T1DM was induced by intraperitoneal injection of streptozotocin (STZ). 1.5 IU insulin was administrated subcutaneously to keep the blood glucose within the normal range. After anesthetizing by isoflurane, the raw data set of pancreatic microcirculation was collected by the multimodal device– and computer algorithm–based microcirculatory evaluating system. After adjusting outliers and normalization, pancreatic microcirculatory oxygen and microhemodynamic data sets were imported into the three-dimensional module and compared.

Results: Microcirculatory profiles of the pancreas in T1DM exhibited a loss of microhemodynamic coherence (significantly decreased microvascular blood perfusion) accompanied by an impaired oxygen balance (significantly decreased PO_2, SO_2, and rHb). More importantly, with insulin administration, the pathological microcirculatory profiles were partially restored. Meanwhile, there were correlations between pancreatic microcirculatory blood perfusion and PO_2 levels.

Conclusions: Our findings establish the first integrated three-dimensional pancreatic microcirculatory profiles of STZ-induced and insulin-administrated T1DM.

KEYWORDS
insulin, microhemodynamics, oxygen, pancreatic microcirculation, type 1 diabetes mellitus

---

---

1 | INTRODUCTION

Type 1 diabetes mellitus (T1DM), with characteristics of hyperglycemia and autoimmune antibodies that destroy the insulin-secreting pancreatic β-cells, is a common chronic metabolic disease. Although the pathophysiological basis of T1DM remains not fully clarified yet, recent findings mentioned the disturbance of pancreatic microcirculation might contribute to the pathogenesis and development of diabetes.[1,2] Microcirculation refers to the terminal vascular network of the systemic circulation consisting of arterioles, capillaries, and venules with diameter <150 μm, which plays a critical role in maintaining the physiological function of organs.[3] Pancreatic microcirculation is a novel concept of great potential significance.[4,5] As a highly vascularized complex,[5] pancreatic microcirculation is responsible for the exchanges of oxygen and nutrient in both endocrine and exocrine and the regulation of glucose metabolic homeostasis through insulin transportation.[6] Maladjustment of pancreatic microcirculation may lead to inadequate nutrient supply in response to glucose variations, which results in consequential pathological phenotype, including T1DM.

It has been already known that heterogeneity in microcirculatory blood perfusion and inadequate transport of oxygen to the microcirculation are closely related to the pathogenesis, and the development of diabetes and its complications.[7] However, the role of oxidative stress and hypoxia in T1DM is still a controversy, especially in the onset of T1DM. It is evident that hyperglycemia in T1DM individuals induces pathological alterations in endothelial cells, which may increase oxidative stress and contribute to endothelial dysfunction.[8] Another etiological theory is that microvasculature engenders hypoxia and ischemia causing the release of biochemical molecules and inflammatory factors,[9] which therefore support the theory that oxidative stress is not an initial causative determinant in the development of T1DM but rather a contributing factor.[10]

Microcirculatory oxygen profile is a crucial issue in microcirculation. It would be more rational and critical to evaluate the functional status of microcirculation via measuring both oxygen and microhemodynamics. The major impediment in understanding the link between pancreatic microcirculatory oxygen profile and T1DM is the inability to see the integrated changes in pancreatic microcirculation, especially during the early stage. Intravital microscope contains considerable application value in the determination of the microcirculatory blood perfusion,[11] measurements reflecting the microcirculatory function more integrally are also recommended. Our group recently released a multimodal device– and computer algorithm–based microcirculatory evaluating approach,[12] which allowed to observe the microhemodynamic and microcirculatory oxygen profiles in the pancreas.

Although recent studies, including ours,[13] have indicated that pancreatic microcirculation is impaired in the development of T1DM, the pathological changes in microcirculatory oxygen profile and microvascular blood perfusion of pancreatic microcirculation remain unknown. Therefore, the aim of the current study was to investigate whether there was loss of microhemodynamic coherence and oxygen imbalance in T1DM and whether insulin administration could alleviate the abnormality of pancreatic microcirculation.

2 | MATERIALS AND METHODS

2.1 | Animals

Animal care and study protocols were approved by the Institutional Animal Care and Use Committee at the Institute of Microcirculation, Chinese Academy of Medical Sciences (CAMS), conducting in accordance with the principles and policies of the Care and Use of Laboratory Animals (IACUC-201709). BALB/c mice (eight weeks old, male) were provided by the Institute of Laboratory Animal Sciences (CAMS, Beijing, China) and were housed five per cage at 26°C and 55% - 70% humidity under 12: 12-h light-dark cycle with diet and water ad libitum.

2.2 | Induction of T1DM model and insulin administration

Eighteen BALB/c mice were assigned to control (n = 6) and streptozotocin (STZ)-injected groups (n = 12) randomly. To induce T1DM, STZ (Sigma-Aldrich, St. Louis, MO), dissolved in 0.1 M citrate buffer (pH =4.3), was intraperitoneally injected into the mice at a dose of 150 mg/kg. The control group received the same volume of 0.1 M citrate buffer. To counteract fatal hypoglycemia following the high dose of STZ injection, 0.25 g/kg glucose saline (Sigma-Aldrich) was given via intraperitoneal route within 5 h after STZ injection (on the experimental day 1) and 10% sucrose water was provided for 72 h (on the experimental days 1–3). From experimental day 4 to day 10, the 10% sucrose water was switched back to regular water until the T1DM models were validated. On the tenth day after STZ injection, fasting blood glucose (FBG) was measured from the tail vein using One Touch UltraEasy® glucometer (LifeScan, Johnson and Johnson, CA) after 6-h fasting. Mice with FBG exceeding 200 mg/dL in two consecutive measurements were considered to be in the onset of T1DM. Six confirmed T1DM mice were administrated with 1.5 IU insulin subcutaneously to keep the blood glucose within the normal range.

2.3 | Hematoxylin-eosin (HE) staining and immunohistochemistry

HE staining was applied to evaluate the morphological changes in pancreatic microcirculation. After fixing with 4% paraformaldehyde, pancreatic tissues were embedded in paraffin and cut into five-micrometer-thick sections for HE staining and immunohistochemical staining. Briefly, sections were deparaffinized, rehydrated, and incubated in boiling 10 mM citrate buffer (pH = 6.0, Zhongshan Golden Bridge Biotechnology, Beijing, China) for

antigen retrieval. And then, sections were incubated with 3% hydrogen peroxide to inhibit endogenous peroxidase, followed by blocking with 3% bovine serum albumin (BSA, TBD Science Technology, Tianjin, China) in phosphate-buffered saline. After incubating with primary mouse monoclonal antibody raised against insulin (2D11-H5) (dilution 1: 50; Santa Cruz Biotechnology, Dallas, TX) and PECAM-1 (dilution 1: 50; Santa Cruz Biotechnology), sections were incubated in blocking buffer overnight at 4°C. Then, horseradish peroxidase–conjugated secondary antibody (Zhongshan Golden Bridge) and 3,3'-diaminobenzidine tetrahydrochloride solution (Zhongshan Golden Bridge) were employed for the incubation of sections, which was monitored on a microscope. Finally, the sections were dehydrated and mounted. Positive staining of insulin and PECAM-1 were determined using a Leica DFC450 microscope (Leica Microsystems, Leitz, Germany).

2.4 | Transmission electron microscopy (TEM)

In order to further investigate the pathological changes in microvessels in the control, type 1 diabetic, and insulin-administrated groups, TEM was subsequently performed. Fresh pancreatic tissues were fixed in 3% buffered glutaraldehyde for 3 h and 1% (w/v) osmic acid for 1 h, followed by dehydration in a graded acetone series and embedding in Epon 812 (SPI, PA, USA). After polymerization of the resin at 60°C for 24 h, ultrathin sections were cut at 70 nm in thickness with ultramicrotome using a diamond knife, stained with 5% uranyl acetate and lead citrate, and observed under a JEM 1230 TEM (JEOL Co., Ltd., Japan). The ultrastructural microvessels in pancreatic microcirculation of three groups were then assessed.

2.5 | Determination of pancreatic microcirculatory profiles

To evaluate the microcirculatory oxygen and microhemodynamic profiles in pancreas, the multimodal device–based microcirculatory evaluating platform was set up (Figure 1), in which the Oxygen to See (O2C, LEA Medizintechnik GmbH, Giessen, Germany), micro fiber-optic oxygen transmitter (Microx TX3, PreSens Precision Sensing GmbH, Regensburg, Germany), and a dual-channel laser Doppler monitoring instrument (VMS-LDF2, Moor Instruments, Ltd., Axminster, UK) were enclosed to determine integrated pancreatic microcirculatory profiles including hemoglobin oxygen saturation (SO_2), the relative amount of hemoglobin (rHb), partial oxygen pressure (PO_2), microvascular blood perfusion, and blood flow velocity.

Briefly, after acclimatizing for 30 min, mice were anesthetized with 2% inhaled isoflurane (R510-22, RWD Life Science Co., Ltd, Shenzhen, China) by small animal anesthesia machine (Matrx VMR, Midmark Corporation, OH) in a 50% mixture of oxygen. The pancreas tissues were exposed by a midline incision, and the probes
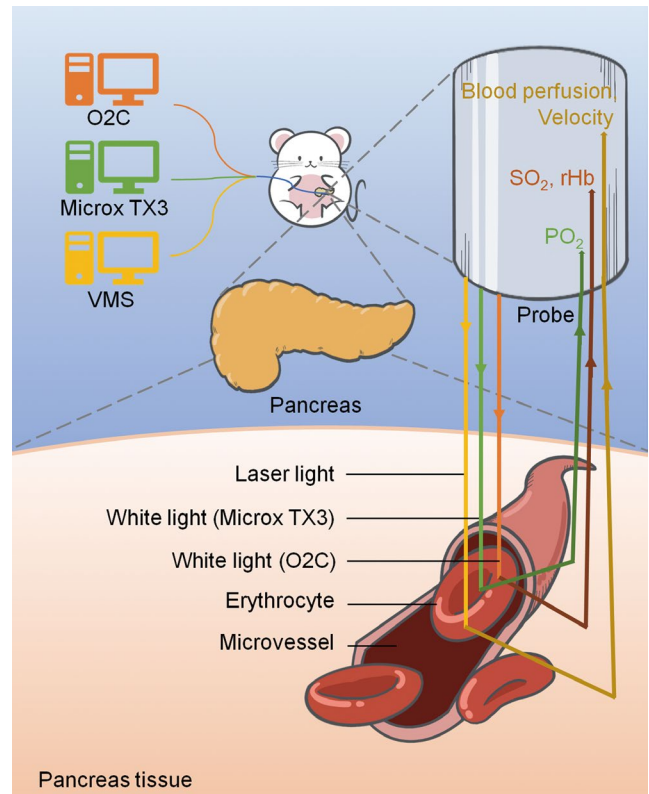
FIGURE 1 Schematic diagram of the multimodal device–based pancreatic microcirculatory profile evaluating platform. The pancreatic microcirculatory oxygen profile (SO_2, rHb, and PO_2) and microhemodynamics were captured by probes of O2C, Microx TX3, and VMS. SO_2, hemoglobin oxygen saturation; rHb, relative amount of hemoglobin; PO_2, partial pressure of oxygen; O2C, Oxygen to See; VMS, dual-channel laser Doppler vascular evaluating system.

were located upon the exposed pancreatic tissue steadily by probe holder (PLT1, Moor Instruments). Pancreatic microcirculatory oxygen data were captured by the O2C and the Microx TX3, respectively. The depth we detected was approximately 1 mm, which was amount to half the depth of probe spacing.[14] Raw data of pancreatic microcirculatory profiles in control, T1DM, and insulin-administrated mice were collected.

2.6 | Construction of three-dimensional (3-D) module of microcirculatory profiles in pancreas

Python (version 3.7.4; https://www.python.org/) and Apache ECharts (version 4.2.0-rc.2; https://echarts.apache.org) under the Apache License (version 2.0; http://www.apache.org/licenses/LICENSE-2.0) were used to generate and visualize the 3-D module of pancreatic microcirculatory profiles. In the 3-D module, we employed the x-axis, y-axis, and z-axis to represent the time course, microcirculatory variables, and calculated microcirculatory values, respectively.

2.7 | Outlier processing

After data capturing with the multimodal device, Python was used to adjust the pancreatic microcirculatory profiles, including SO_2, rHb, PO_2, blood perfusion, and velocity. At the stage of preprocessing, the outliers of microcirculatory oxygen and microhemodynamic data sets were identified and processed by box plot algorithm. We defined Q_1 as the 25th percentile largest value and Q_3 as the 75th percentile largest value. The difference between Q_3 and Q_1 was interquartile range (IQR). Microcirculatory values exceeding the range from ($Q_1 - 1.5 \times IQR$) to ($Q_3 + 1.5 \times IQR$) were classified as outliers and adjusted to the nearest boundary value.

2.8 | Integration of pancreatic microcirculatory oxygen and microhemodynamic data sets

To unify the microcirculatory oxygen and microhemodynamic data sets of pancreatic microcirculatory profiles into the 3-D module, the time granularity was transformed by method of the least common multiple algorithms. Additionally, considering the different units of data set, the min-max normalization was performed to adjust the dimensions of microcirculatory data set in the 3-D module.

The min-max normalization is calculated as follows:

$$x' = \frac{x - min}{max - min} \qquad (1)$$

where x is the original microcirculatory data of pancreas, and x' represents the data with normalization. Min value is the minimum value of microcirculatory oxygen and microhemodynamic data, while max value refers to the maximum value.

2.9 | Video recording of dynamic 3-D modules of microcirculatory profiles in pancreas

In order to visualize dynamic 3-D modules of microcirculatory profiles of control and T1DM mice with or without insulin administration in pancreas, ScreenToGif (version 2.19.3; URL: https://www.screentogif.com/) was used to record the dynamic 3-D modules of the control, T1DM, and insulin-administrated groups, respectively. Length of approximately 1 min of each video was saved in format of MP4. The bit rate of the video was approximately 200 Kbps with 1176 × 594 in resolution ratio.

2.10 | Statistical analysis

Statistical analyses were performed using the SPSS software (version 21.0; IBM, Armonk, NY). All microcirculatory signals and transformed data of pancreatic microcirculatory profiles were expressed as mean ±standard deviation (SD). Data set was subjected to the t test (between two groups), and one-way analysis of variance (ANOVA) was performed for multiple comparisons among the three groups. Furthermore, the correlations between microcirculatory oxygen profile and microhemodynamic data sets were analyzed with Pearson's correlation coefficients (r) using the GraphPad Prism (version 8.0.2; GraphPad Software, San Diego, CA) and were considered relevant for associated $p < 0.05$ and correlation coefficient values of $r > 0.4$ or $r < 0.4$.

3 | RESULTS

3.1 | Identification of STZ-induced T1DM mouse model

The type 1 diabetic mice induced by STZ showed a higher level of FBG than those in the control group. Induction of the T1DM model was characterized by a significant increase in FBG and decrease in body weight (Figure 2). As expected, it was noted that the blood glucose level was higher in type 1 diabetic mice than in the insulin-administrated group (Figure 2A), and the body weight of mice in the T1DM group was significantly lower than that of mice in the control group and insulin-administrated group (Figure 2B). HE staining, immunohistochemistry labeling of insulin and endothelial marker PECAM-1 (CD31), and TEM revealed pancreatic microcirculatory morphological abnormalities in T1DM mice (Figure 2C-2F). Taken together, these findings suggested that T1DM mouse model was successfully established by 150 mg/kg STZ injection.

3.2 | 3-D module of microcirculatory profiles

To characterize integrated microcirculatory oxygen and microhemodynamic profiles in pancreas, the raw data set with preprocessing was substituted into the original coordinate axis of 3-D modules, including microcirculatory SO_2, rHb, PO_2, blood perfusion, and velocity. In the 3-D module, histograms were employed to display the tendency of pancreatic microcirculatory data set of control (Figure 3A, 3B, Video S1; all supplemental materials are available at https://figshare.

FIGURE 2 Comparisons of fasting blood glucose and body weight of control, STZ-induced type 1 diabetic, and insulin-administrated mice. The type 1 diabetic mouse model was induced by STZ induction, which exhibited abnormal fasting blood glucose (A) and body weight (B). Data are presented as mean ±SD. Control, $n = 6$; T1DM, $n = 6$; insulin-administrated, $n = 6$. * $p < 0.05$, ** $p < 0.01$, *** $p < 0.001$, **** $p < 0.0001$. 23434: Hematoxylin-eosin (HE) staining of the pancreatic microcirculation in the control, T1DM, and insulin-administrated groups. Representatives of pancreatic microvasculature (arrow) are illustrated. Scale bar =50 μm. D: Immunohistochemical staining of insulin in three groups. Scale bar =50 μm. E: Immunohistochemical staining of PECAM-1 in three groups. Scale bar =50 μm. Arrows indicate microvessels. The inserts revealed enlarged microvessels in pancreatic microcirculation. Scale bar =20 μm. F: Ultrastructure of pancreatic microcirculation revealed by TEM. Magnification =2000×. Arrows indicate microvessels of pancreatic microcirculation. Scale bar =5 μm. Control, control mice; T1DM, STZ-induced type 1 diabetic mice without insulin administration; insulin-administrated, STZ-induced diabetic mice with 1.5 IU insulin administration. T1DM, type 1 diabetes mellitus; STZ, streptozotocin; HE, hematoxylin-eosin; TEM, transmission electron microscopy.

**(A)** through **(F)** figure panels.
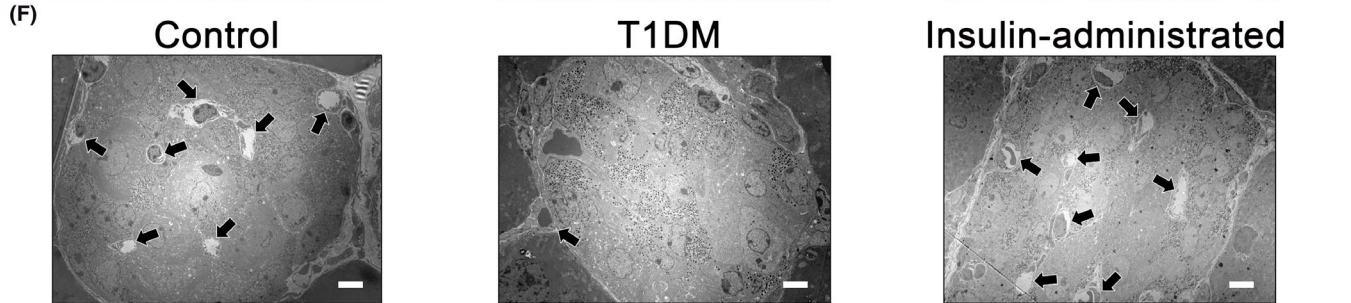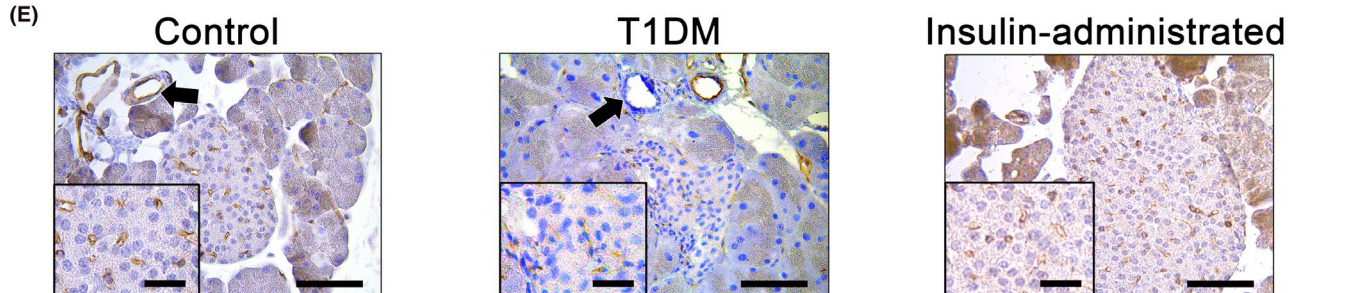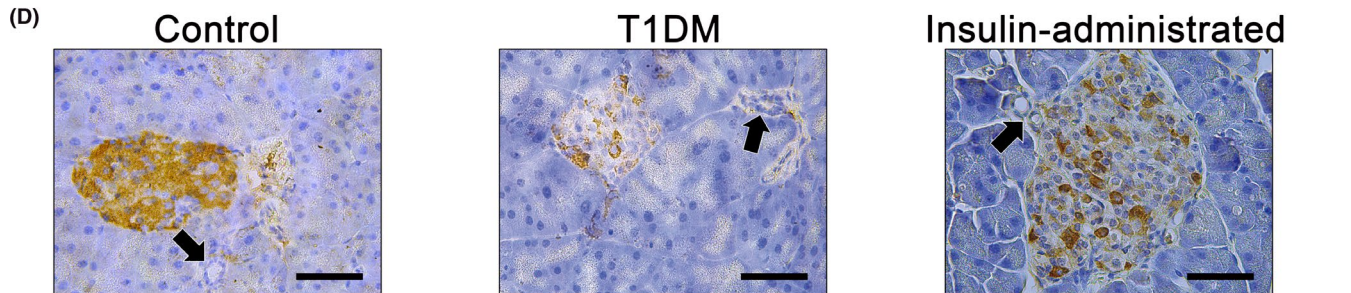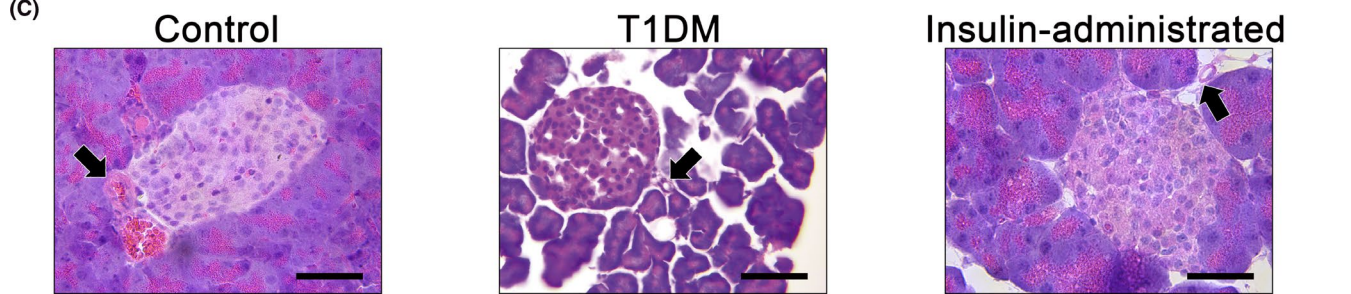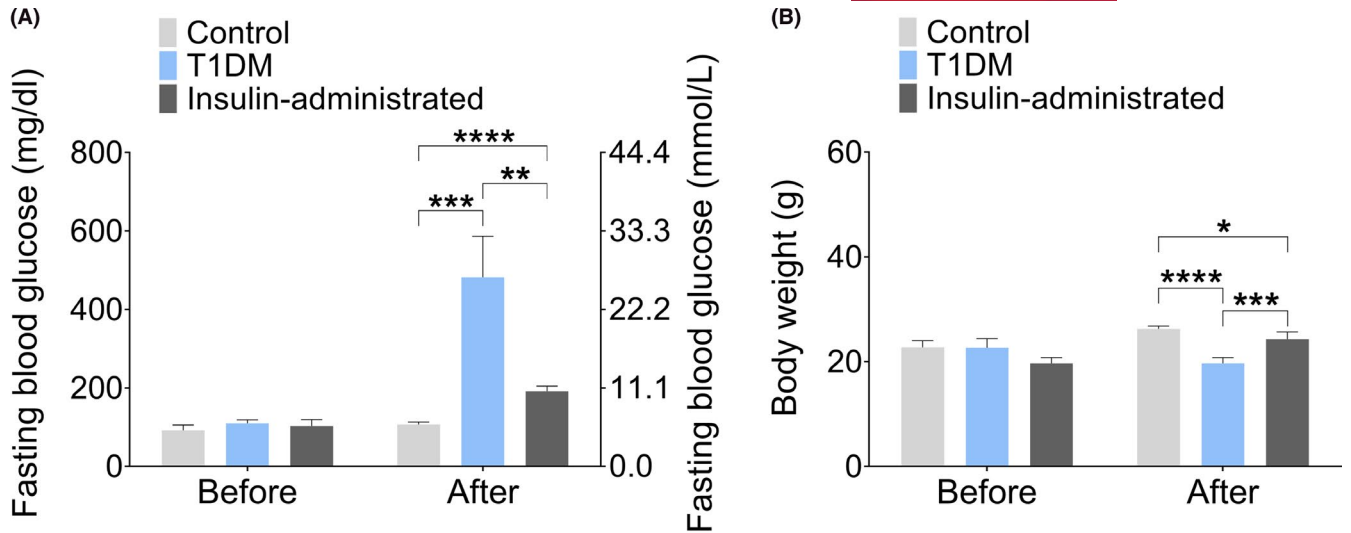
com/s/892060bbbf890c63d739), T1DM (Figure 4A, 4B, Video S2), and insulin-administrated (Figure 5A, 5B, Video S3) groups, while scatter plots were applied to show the distribution of microcirculatory profiles (Figure 3C, 3D; Figure 4C, 4D; Figure 5C, 5D; Video S4–6). It was noted that both pancreatic microcirculatory oxygen and microhemodynamics were oscillated.

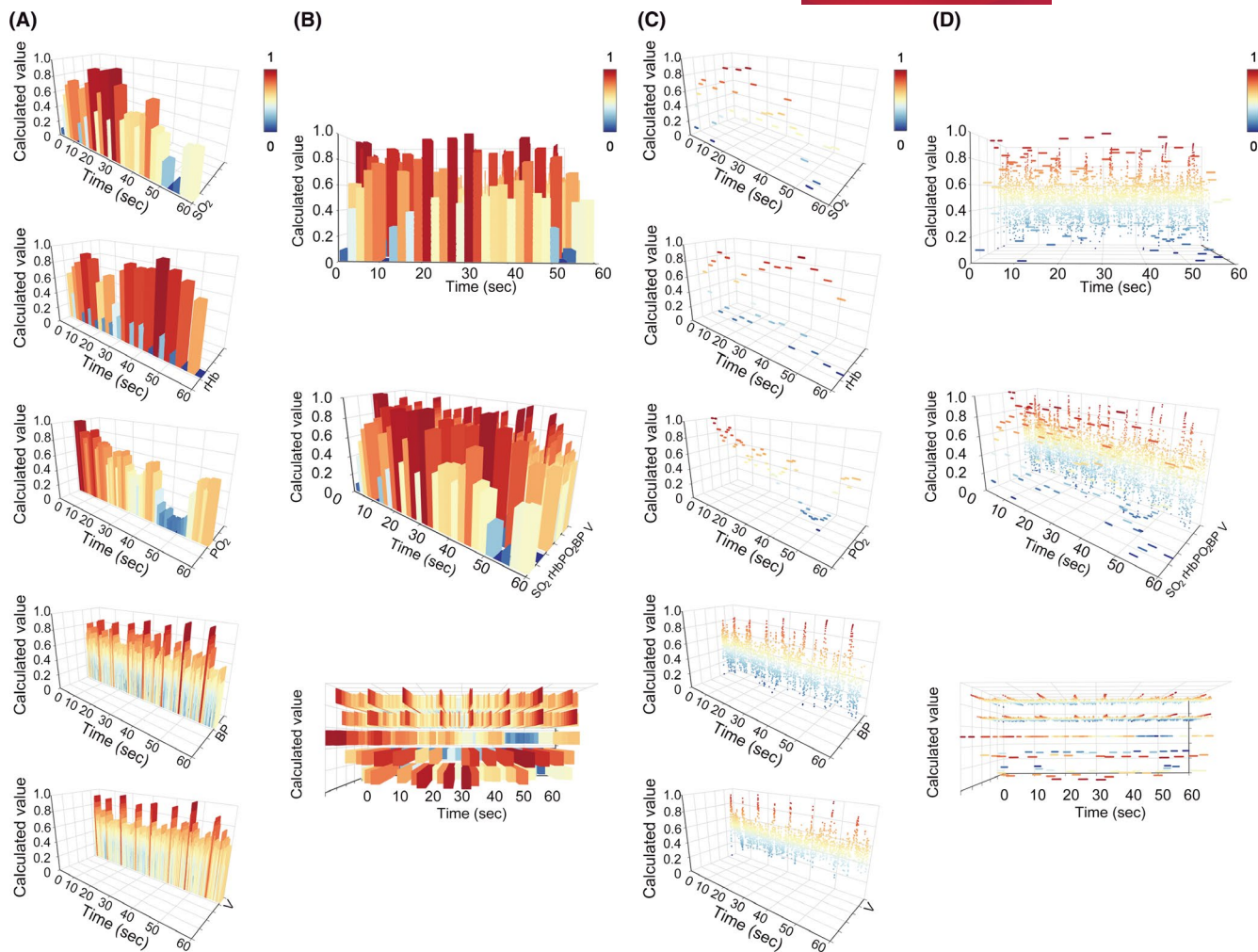## 3.3 | Decreased pancreatic microcirculatory oxygen profile in T1DM

Using the multimodal device–based pancreatic microcirculatory profile evaluating platform, we captured microcirculatory oxygen data set, including the SO_2, rHb, and PO_2 in pancreas (Figure 6). The loss of microcirculatory oxygen in pancreatic microcirculatory network was observed in T1DM. As shown in Figure 6A and Figure 6D, the SO_2 level in pancreatic microcirculation of T1DM mice (86.68% ±3.19%) was significantly lower than that of control mice (93.03% ±4.41%), an approximate 6.8% reduction in SO_2 level in T1DM mice was revealed. The pancreatic microcirculatory rHb level is displayed in Figure 6B and Figure 6E. The rHb level of T1DM group (60.84 AU ±4.30 AU; AU, arbitrary unit) exhibited a decline compared with the control group (63.20 AU ±5.74 AU). However, as shown in Figure 6E, the rHb level displayed a significant increase with the presence of insulin administration (60.48 AU ±6.57 AU). After insulin administration, the pancreatic microcirculatory rHb showed a comparable level compared with the control mice.

Furthermore, the microcirculatory oxygen profile in pancreatic capillaries exhibited a broad dynamic distribution in the range from 36.6 hPa to 44.5 hPa under type 1 diabetic pathological condition.
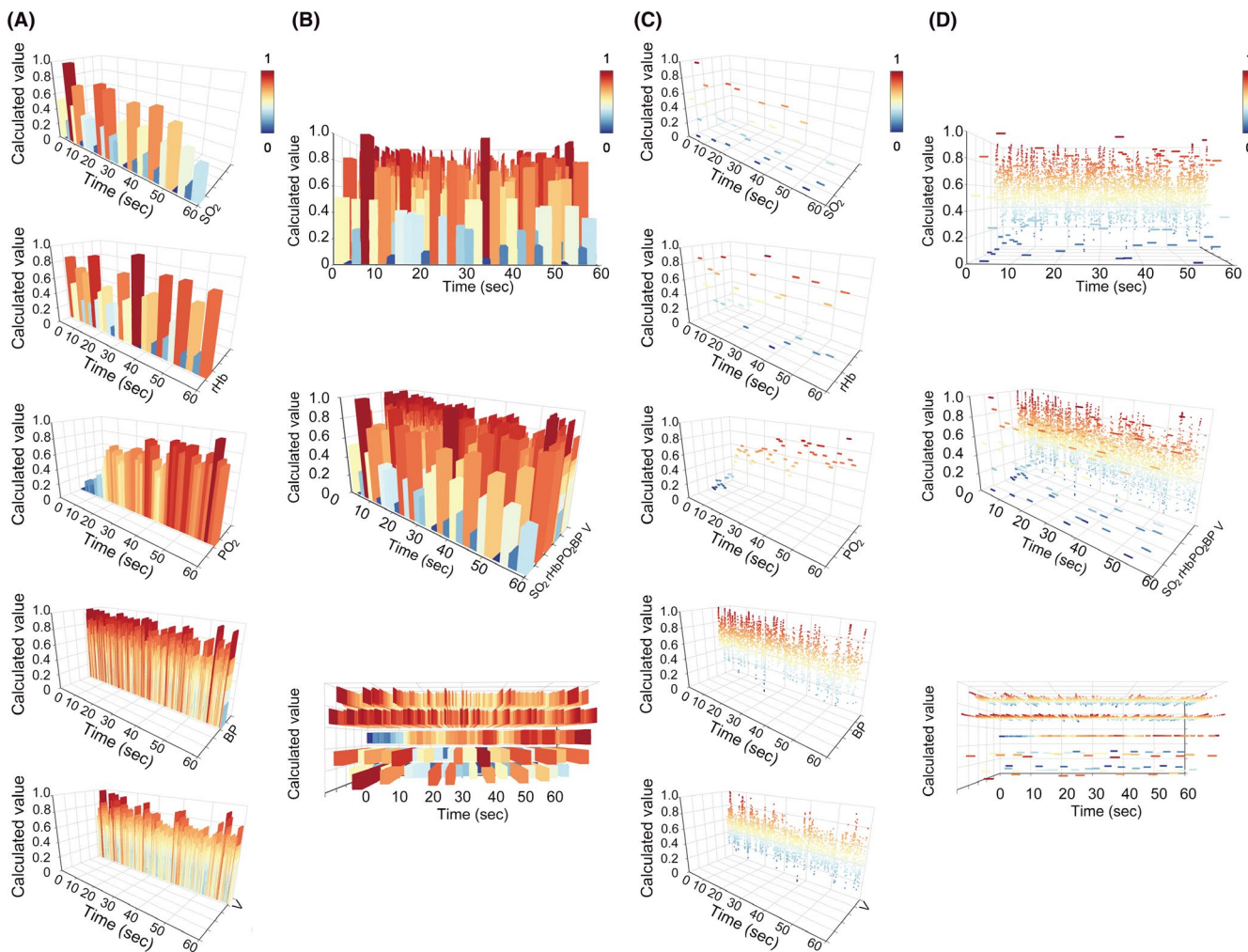
FIGURE 3 Three-dimensional (3-D) module of pancreatic microcirculatory profiles in control mice. A: Separated 3-D module of microcirculatory oxygen profile (SO_2, rHb, and PO_2) and microhemodynamics (microvascular blood perfusion and velocity). B: Front view, side view (rotated 45° toward left), and overlook view (rotated 90° toward down) of the 3-D module of improved pancreatic microcirculatory profiles. C: Separated scattered 3-D module of microcirculatory oxygen profile and microhemodynamics. D: Front view, side view (rotated 45° toward left), and overlook view (rotated 90° toward down) of the scattered 3-D module. T1DM, type 1 diabetes mellitus; SO_2, oxygen saturation; rHb, relative amount of hemoglobin; PO_2, partial oxygen pressure; 3-D, three-dimensional.

FIGURE 4 Abnormality of three-dimensional (3-D) module of pancreatic microcirculatory profiles in the T1DM group. A: Separated 3-D module of microcirculatory oxygen profile (SO_2, rHb, and PO_2) and microhemodynamics (microvascular blood perfusion and velocity). B: Front view, side view (rotated 45° toward left), and overlook view (rotated 90° toward down) of the 3-D module of improved pancreatic microcirculatory profiles. C: Separated scattered 3-D module of microcirculatory oxygen profile and microhemodynamics. D: Front view, side view (rotated 45° toward left), and overlook view (rotated 90° toward down) of the scattered 3-D module. T1DM, type 1 diabetes mellitus; SO_2, oxygen saturation; rHb, relative amount of hemoglobin; PO_2, partial oxygen pressure; 3-D, three-dimensional.
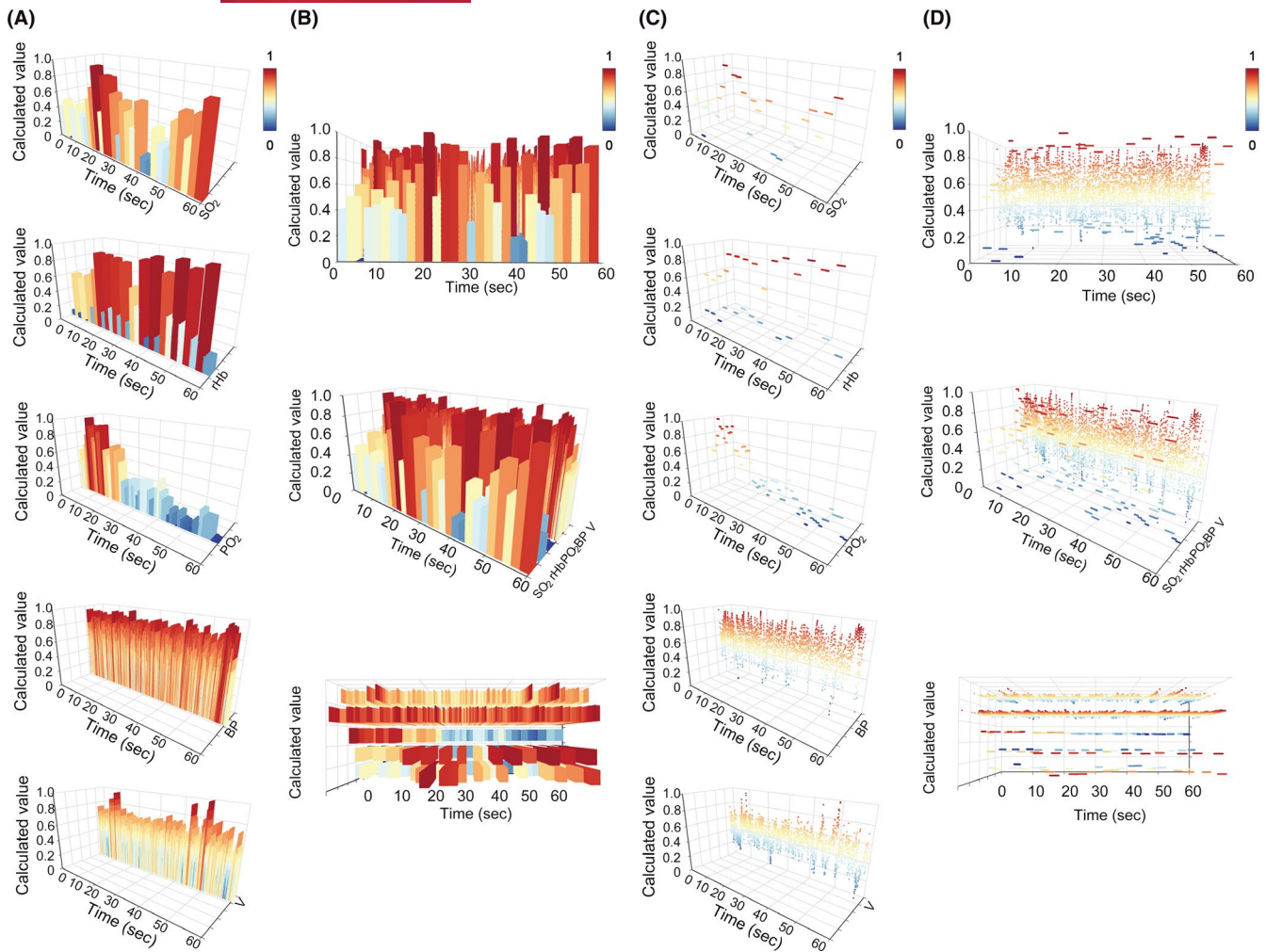
In Figure 6C, the pancreatic microcirculatory PO_2 levels of both the T1DM mice (39.90 hPa ±1.69 hPa) and the insulin-administrated mice (55.41 hPa ±10.08 hPa) were lower than control (62.74 hPa ±1.99 hPa). Insulin administration increased 38.9% in PO_2 level compared with the T1DM group (Figure 6F).

3.4 | Abnormalities of pancreatic microhemodynamics

The pancreatic microhemodynamic data set was then visualized and analyzed (Figure 7). Interestingly, the pancreatic microvascular blood perfusion and velocity showed the same responses to the respective pathophysiological conditions. The microvascular blood perfusion level (791.98 PU ±100.36 PU; PU, perfusion unit) was

significantly decreased upon type 1 diabetic status as compared to control (902.66 PU ±78.50 PU) and was alleviated during insulin administration (823.29 PU ±101.56 PU).

In addition, the tendency of microcirculatory velocity was similar to that of microvascular blood perfusion among the control, T1DM, and the insulin-administrated groups (Figure 7C-7D). Concordantly, compared with the control group (135.46 PU ±15.52 PU), STZ injection increased the microcirculatory blood perfusion velocity of the T1DM group (142.41 PU ±16.75 PU) by 5.1%. The velocity of insulin-administrated mice was reduced by 2.6% as opposed to T1DM without insulin administration. Taken together, STZ-induced type 1 diabetic pathological condition exhibited a reduced pancreatic microcirculatory oxygen and microhemodynamics, while a comprehensive pancreatic microcirculatory protective effect of insulin administration in T1DM was observed.

FIGURE 5 Improvement in three-dimensional (3-D) module of pancreatic microcirculatory profiles in insulin-administrated mice. *A*: Separated 3-D module of microcirculatory oxygen profile (SO_2, rHb, and PO_2) and microhemodynamics (microvascular blood perfusion and velocity). *B*: Front view, side view (rotated 45° toward left), and overlook view (rotated 90° toward down) of the 3-D module of improved pancreatic microcirculatory profiles. *C*: Separated scattered 3-D module of microcirculatory oxygen profile and microhemodynamics. *D*: Front view, side view (rotated 45° toward left), and overlook view (rotated 90° toward down) of the scattered 3-D module. T1DM, type 1 diabetes mellitus; SO_2, oxygen saturation; rHb, relative amount of hemoglobin; PO_2, partial oxygen pressure; 3-D, three-dimensional.

3.5 | Correlation analysis between pancreatic microcirculatory oxygen profile and microhemodynamics

To investigate whether there was uncoupling microcirculatory oxygen demand from microvascular blood perfusion, we next analyzed the correlations between pancreatic microcirculatory oxygen and microhemodynamic profiles. As demonstrated in Figure 8A,D, it was revealed that a significant positive correlation was found between microcirculatory PO_2 and blood perfusion within control mice ($r = 0.686$, $p < 0.0001$), while a negative correlation was found between PO_2 and microvascular blood perfusion ($r = -0.628$, $p < 0.001$) in the T1DM mice. Moreover, after insulin administration, positive correlation was reappeared between PO_2 and blood perfusion ($r = 0.680$, $p < 0.0001$). The abnormalities of integrated pancreatic microcirculation in T1DM mice were further supported by the negative correlation between PO_2 and velocity in T1DM mice ($r = -0.746$, $p < 0.0001$). However,

with regard to SO_2, no significant correlations between pancreatic microcirculatory oxygen profile and microhemodynamics were found among three groups (Figure 8B, control group: $r = -0.0227$, $p = 0.905$; T1DM group: $r = -0.01691$, $p = 0.929$; and insulin-administrated group: $r = 0.255$, $p = 0.1748$). Consistent with SO_2, no significant correlations between rHb and blood perfusion were found (Figure 8C, control group: $r = -0.115$, $p = 0.5463$; T1DM group: $r = -0.094$, $p = 0.6213$; and insulin-administrated group: $r = -0.047$, $p = 0.8048$). These data suggest that toward T1DM, blood-oxygen transportation in integrated pancreatic microcirculation was imbalanced.

4 | DISCUSSION

The changes in microcirculation in the etiopathogenesis of T1DM have been highlighted in a series of studies over decades.[15,16] In the current study, we released the first integrated STZ-induced
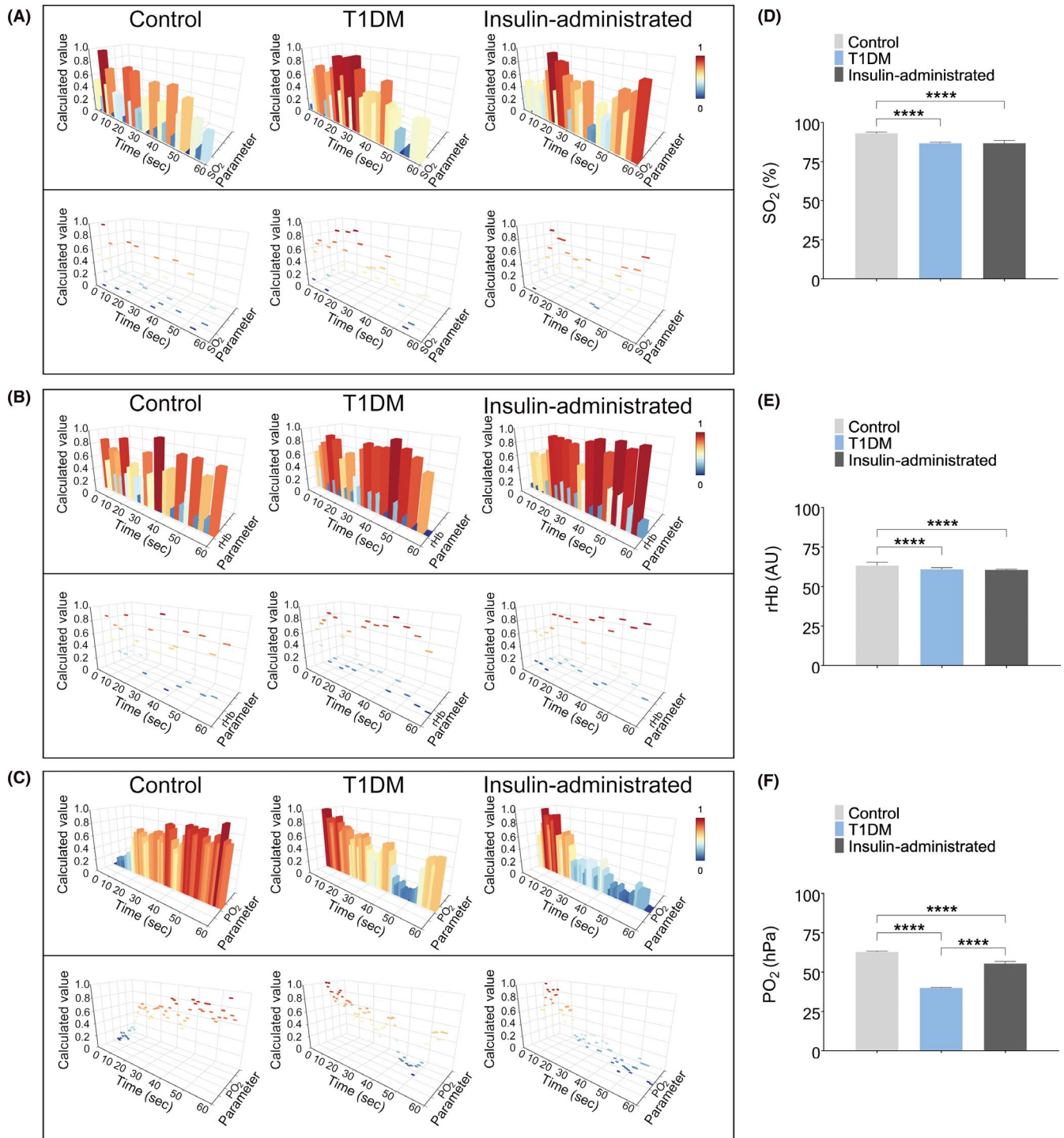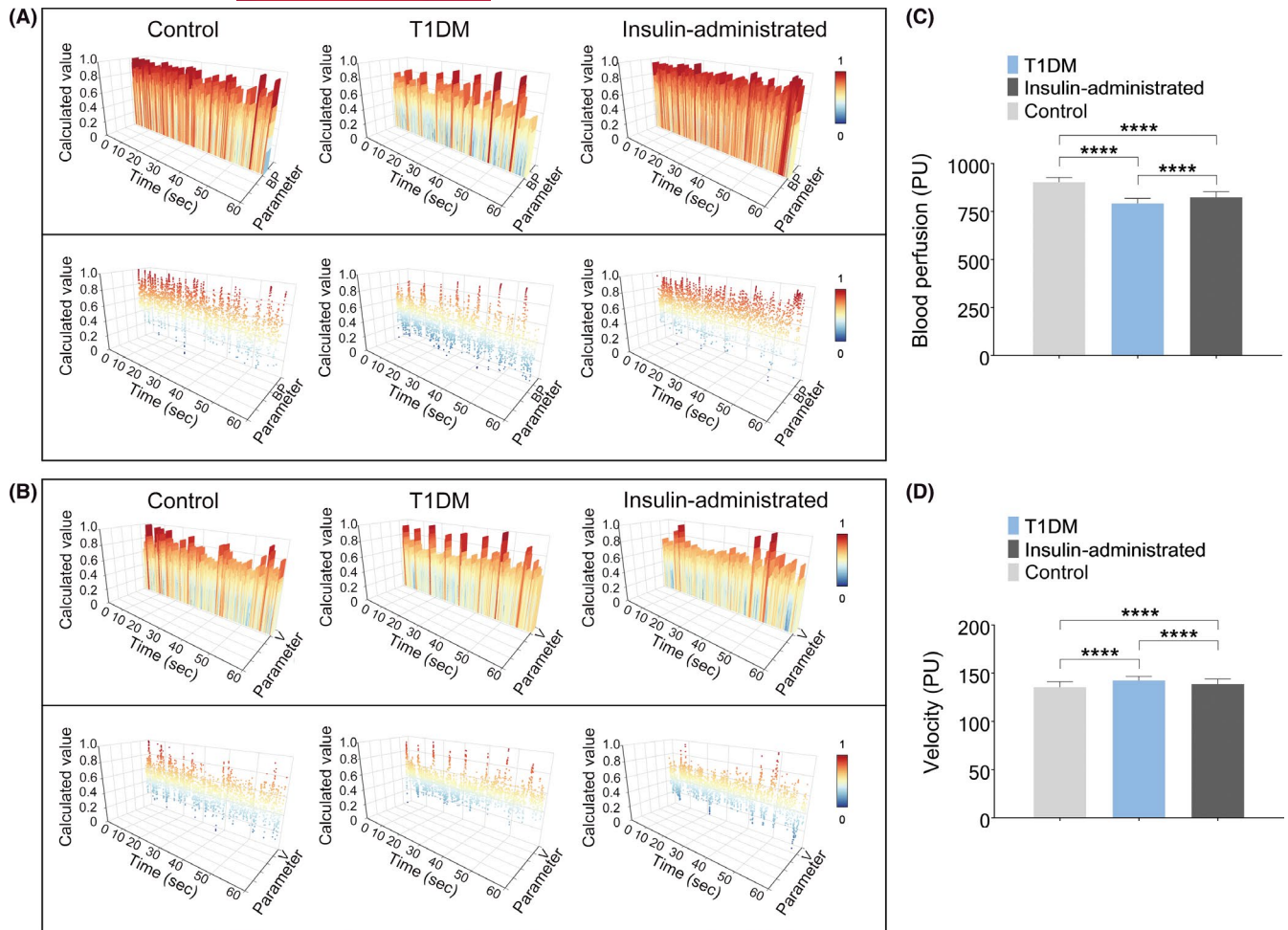
FIGURE 6 Integrated analysis of microcirculatory oxygen profile of pancreatic microcirculation. (A-C) Separate coordinates of pancreatic microcirculatory oxygen profile. (D-F) Comparisons of SO_2, rHb, and PO_2 levels in control and T1DM mice with or without insulin administration. Control, control mice; T1DM, STZ-induced type 1 diabetic mice without insulin administration; insulin-administrated, STZ-induced diabetic mice with 1.5 IU insulin administration. Control, $n = 6$; T1DM, $n = 6$; insulin-administrated, $n = 6$. **** $p < 0.0001$. T1DM, type 1 diabetes mellitus; STZ, streptozotocin; SO_2, oxygen saturation; rHb, relative amount of hemoglobin; PO_2, partial oxygen pressure; AU, arbitrary unit; 3-D, three-dimensional.

and insulin-administrated T1DM pancreatic microcirculatory profiles using the multimodal device– and computer algorithm–based pancreatic microcirculatory evaluating system. Furthermore, we demonstrated that microcirculatory oxygen profile and microhemodynamics of pancreas were deteriorated in the onset of T1DM.

As a crucial unit for information and material exchange, pancreatic microcirculation plays a key role in maintaining normal physiological function and homeostasis of internal environment through distribution of oxygenated blood flow to meet the metabolic demand.[17-19] The supply of oxygen to tissues is generally controlled by microcirculatory

FIGURE 7 Integration of microcirculatory hemodynamics of pancreatic microcirculation. (A, B) Separate coordinates of pancreatic microhemodynamics. (C, D) Comparisons of pancreatic microvascular blood perfusion and velocity in control and T1DM mice with or without insulin administration. Control, control mice; T1DM, STZ-induced type 1 diabetic mice without insulin administration; insulin-administrated, STZ-induced diabetic mice with 1.5 IU administration. Control, $n = 6$; T1DM, $n = 6$; insulin-administrated, $n = 6$. **** $p < 0.0001$. T1DM, type 1 diabetes mellitus; STZ, streptozotocin; PU, perfusion unit; 3-D, three-dimensional.

blood flow.[20] Earlier studies mentioned that pancreatic islets receive ~15% of blood perfusion despite occupying only 1% of total pancreatic mass.[21] Our result offers a pathological phenotype that integrated pancreatic microcirculatory dysfunction is implicated in T1DM. It could be speculated that impairments in both the structural and functional profiles of pancreatic microcirculation may result in lower oxygen supply due to decreased pancreatic microvascular blood perfusion.

Generally, PO_2 is the marker representing the balance between oxygen supply and metabolic demand. In red blood cells, approximately 98% of the oxygen in arterial blood is carried in the bound form by hemoglobin. The fluctuation in PO_2 was defined as erythrocyte-related transients and a manifestation of the microcirculatory adjustment to oxygen transport.[22] In agreement with the pathological phenotype, there was a strong positive association

FIGURE 8 Correlation analysis among pancreatic microcirculatory oxygen and microhemodynamic profiles. A: Correlation coefficients in control, T1DM, and insulin-administrated groups. Numbers in the figure represent correlation coefficient r value. B-D: Correlations between pancreatic microcirculatory oxygen profile and microvascular blood perfusion in the control, T1DM, and insulin-administrated groups. B: No correlations between microcirculatory SO_2 and microvascular blood perfusion were found among the groups. C: Pancreatic microcirculatory rHb was not associated with pancreatic microvascular blood perfusion. D: Positive correlation between microcirculatory PO_2 and microvascular blood perfusion was found in both control ($r = 0.686$, $p < 0.0001$) and insulin-administrated ($r = 0.680$, $p < 0.0001$) groups. Negative correlation between microcirculatory PO_2 and microvascular blood perfusion was found in T1DM mice ($r = -0.628$, $p = 0.0002$). Blue circle represents control mice. Red triangle represents the T1DM group without insulin administration. Green rectangle represents T1DM administrated with insulin. Control, control mice; T1DM, STZ-induced type 1 diabetic mice without insulin administration; insulin-administrated, STZ-induced diabetic mice with 1.5 IU administration. Control, $n = 6$; T1DM, $n = 6$; insulin-administrated, $n = 6$. * $p < 0.05$, *** $p < 0.001$, **** $p < 0.0001$. T1DM, type 1 diabetes mellitus; STZ, streptozotocin; SO_2, oxygen saturation; rHb, relative amount of hemoglobin; PO_2, partial oxygen pressure; AU, arbitrary unit; PU, perfusion unit.

(A)

(B)

(C)

(D)
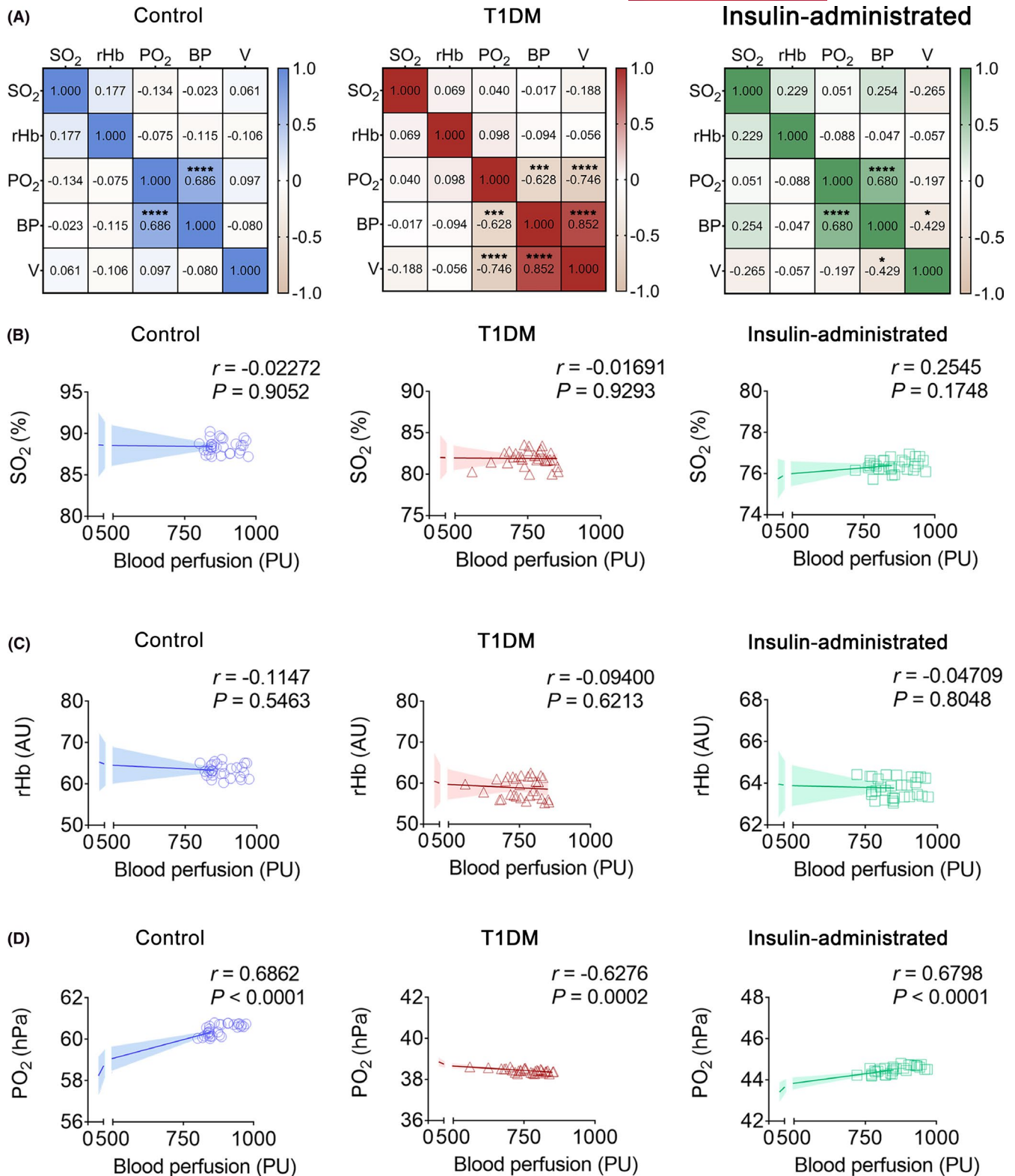
between the pancreatic microcirculatory PO_2 and microvascular blood perfusion in control and insulin-administrated groups. And importantly, the blood-oxygen correlation was markedly inversed in T1DM mice. The loss of microcirculatory PO_2 level in the pancreatic microvasculature network during the onset of T1DM, which is associated with vascular endothelial growth factor,[13,23,24]

reflects the reduction in dissolved oxygen in pancreas tissues in the development of T1DM.

Prediabetes induces dysregulation of microvasculature altering red blood cell-capillary interaction leading to activation of hypoxia signaling pathways.[25] Experimental data on the integrated microcirculatory oxygen profile of pancreas are scarce. Besides PO_2, our

results further demonstrate that there is a dramatic decrease in rHb and SO_2 even in the onset of T1DM, which may be explained by the oxygen metabolic rate.[26] In addition, the changes in microhemodynamics occurred parallel to the variation in microcirculatory oxygen profile. On the other hand, microcirculation is not only a crucial component for the response to hypoxia-induced dynamic changes but also the central component in which hypoxia-mediated pathophysiological effects are generated. In diabetic retinopathy, it has been demonstrated that complications in retinal oxygen metabolism may occur before the changes in the retinal microvasculature.[27] Furthermore, hypoxia-induced pancreatic microcirculatory stellate cell activation contributes to the β-cell loss.[28] This finding indicates that the integrated pancreatic microcirculatory profiles have the potential to be a good index for evaluating pancreatic dysfunction in T1DM.

Without intervention, the early stage of T1DM will progress to overt T1DM, which is associated with undesirable clinical outcomes.[29] Based on our microcirculatory data set, correcting and controlling hyperglycemia is not entirely effective at restoring physiological cellular metabolism and function. Cytoprotective agents are introduced to alleviate hypoxia-induced islet dysfunction. Administration of curcumin,[30] metformin,[31] and insulin[32] has been proved to prevent β-cell apoptosis by suppressing ROS elevation. Therefore, it is believed that the integrated microcirculatory theory targeted at improving microcirculation would achieve better objective curative effects. Furthermore, except for blood glucose management, administration of microcirculation-improving drugs that prevent the individuals with the early stage of T1DM from progressing to mild and severe stages of T1DM might be a strategy unless otherwise contraindicated.

Microcirculatory endothelial dysfunction can occur very early in T1DM individuals, that is, before the occurrence of overt vascular complications.[8] Our recent data have demonstrated that mitochondrial ultrastructural morphology of pancreatic microvascular endothelial cell is abnormal in T1DM mice.[32] Furthermore, it has been proved that nitric oxide is closely associated with the convective oxygen supply through its vasodilation characteristics,[33] and has the capability to modulate oxygen consumption by mitochondria.[34] Hence, understanding of pancreatic microcirculatory oxygenation distribution may benefit the interpretation of blood-oxygen level and the role of microcirculation in the development of T1DM.

Pancreatic microcirculatory oxygen profile in diabetic pathological condition has been investigated for decades. However, the notion of oxygen loss has been questioned due to methodological limitations, as well as a lack of understanding of the relations between microcirculation and the novel view of microcirculatory oxygen-blood contribution to T1DM. Techniques are attempted to explore the integrated microcirculatory function aiming at the inherent characteristics of microvascular hemodynamic and oxygen profiles. As such, the heterogeneity and variability of microcirculation are suggested that should be considered regarding the link between microcirculation and the conventional theory of diabetes. Our pancreatic microcirculatory evaluating system made it possible to assess the integrated microcirculatory oxygen profile in pancreas, which can provide information on the capability of oxygen delivery to address pancreatic metabolic demand, as well as to optimize perfusion and oxygenation, and visualize and quantify integrated pancreatic microcirculatory profiles allowing individualized treatment strategies for T1DM. We believe that our data set in combination with microvascular blood perfusion and microcirculatory oxygen profiles will provide the comprehensive evidence for further understanding the roles of integrated pancreatic microcirculation in T1DM.

5 | CONCLUSION

Monitoring of STZ-induced and insulin-administrated pancreatic microcirculatory profiles (including microcirculatory oxygen profile and microhemodynamics) during the development of T1DM was performed with the assistance of the multimodal device– and computer algorithm–based evaluating platform. In the onset of T1DM, the pancreatic microcirculatory oxygen and microhemodynamic profiles became abnormal and therefore have the potential to serve as an indicator for revealing pancreatic dysfunction, providing an underlying certain value in clinical and academic research.

6 | PERSPECTIVES

- Using the multimodal device– and computer algorithm–based microcirculatory monitoring platform, we established three-dimensional integrated pancreatic microcirculatory profiles of STZ-induced and insulin-administrated T1DM.
- In the onset of T1DM, the pancreatic microcirculatory oxygen and microhemodynamic profiles became abnormal and therefore have the potential to serve as an indicator for revealing pancreatic microcirculatory dysfunction, providing an underlying certain value in clinical and academic research.
- The loss of pancreatic microhemodynamic coherence is accompanied by an imbalanced microcirculatory oxygen exhibiting in the onset of T1DM, which could be partially restored by insulin administration.

CONFLICT OF INTEREST

The authors declare no conflict of interest.

ORCID

Yuan Li https://orcid.org/0000-0002-0065-9038

Bingwei Li https://orcid.org/0000-0002-0373-446X

Bing Wang https://orcid.org/0000-0002-7287-0852

Mingming Liu https://orcid.org/0000-0002-6750-5068

Xiaoyan Zhang https://orcid.org/0000-0002-4725-1849

Ailing Li https://orcid.org/0000-0003-4937-4700

Jian Zhang https://orcid.org/0000-0001-5616-7297

Honggang Zhang https://orcid.org/0000-0002-6837-8443

Ruijuan Xiu https://orcid.org/0000-0002-1446-2711

REFERENCES

1. Inanc M, Tekin K, Kiziltoprak H, et al. Changes in retinal microcirculation precede the clinical onset of diabetic retinopathy in children with type 1 diabetes mellitus. *Am J Ophthalmol*. 2019;207:37-44.
2. Jansson L, Barbu A, Bodin B, et al. Pancreatic islet blood flow and its measurement. *Ups J Med Sci*. 2016;121:81-95.
3. Gutterman DD, Chabowski DS, Kadlec AO, et al. The human microcirculation: regulation of flow and beyond. *Circ Res*. 2016;118:157-172.
4. Dybala MP, Gebien LR, Reyna ME, et al. Implications of integrated pancreatic microcirculation: crosstalk between endocrine and exocrine compartments. *Diabetes*. 2020;69:2566-2574.
5. Dybala MP, Kuznetsov A, Motobu M, et al. Integrated pancreatic blood flow: bidirectional microcirculation between endocrine and exocrine pancreas. *Diabetes*. 2020;69:1439-1450.
6. Ellis CG, Jagger J, Sharpe M. The microcirculation as a functional system. *Crit Care*. 2005;9(Suppl 4):S3-S8.
7. Resanovic I, Zaric B, Radovanovic J, et al. Hyperbaric oxygen therapy and vascular complications in diabetes mellitus. *Angiology*. 2020;71:876-885.
8. Ceriello A, Kumar S, Piconi L, et al. Simultaneous control of hyperglycemia and oxidative stress normalizes endothelial function in type 1 diabetes. *Diabetes Care*. 2007;30:649-654.
9. Howangyin KY, Silvestre JS. Diabetes mellitus and ischemic diseases: molecular mechanisms of vascular repair dysfunction. *Arterioscler Thromb Vasc Biol*. 2014;34:1126-1135.
10. Gerber PA, Rutter GA. The role of oxidative stress and hypoxia in pancreatic beta-cell dysfunction in diabetes mellitus. *Antioxid Redox Signal*. 2017;26:501-518.
11. Hutchings S, Watts S, Kirkman E. The Cytocam video microscope. A new method for visualising the microcirculation using Incident Dark Field technology. *Clin Hemorheol Microcirc*. 2016;62:261-271.
12. Li Y, Song X, Liu M, et al. Multimodal device and computer algorithm-based monitoring of pancreatic microcirculation profiles in vivo. *Pancreas*. 2020;49:1075-1082.
13. Liu M, Zhang X, Li A, et al. Insulin treatment restores islet microvascular vasomotion function in diabetic mice. *J Diabetes*. 2017;9:958-971.
14. Meglinsky IV, Matcher SJ. Modelling the sampling volume for skin blood oxygenation measurements. *Med Biol Eng Comput*. 2001;39:44-50.
15. Wasserman DH, Wang TJ, Brown NJ. The vasculature in prediabetes. *Circ Res*. 2018;122:1135-1150.
16. Neubauer-Geryk J, Kozera GM, Wolnik B, et al. Decreased reactivity of skin microcirculation in response to L-arginine in later-onset type 1 diabetes. *Diabetes Care*. 2013;36:950-956.
17. Saldivar E, Cabrales P, Tsai AG, et al. Microcirculatory changes during chronic adaptation to hypoxia. *Am J Physiol Heart Circ Physiol*. 2003;285:H2064-H2071.
18. Diesen DL, Hess DT, Stamler JS. Hypoxic vasodilation by red blood cells: evidence for an s-nitrosothiol-based signal. *Circ Res*. 2008;103:545-553.
19. Popel AS, Johnson PC. Microcirculation and hemorheology. *Annu Rev Fluid Mech*. 2005;37:43-69.
20. Premont RT, Stamler JS. Essential role of hemoglobin betaCys93 in cardiovascular physiology. *Physiology (Bethesda)*. 2020;35:234-243.
21. Komatsu H, Kandeel F, Mullen Y. Impact of oxygen on pancreatic islet survival. *Pancreas*. 2018;47:533-543.
22. Pittman RN. Oxygen transport in the microcirculation and its regulation. *Microcirculation*. 2013;20:117-137.
23. Schlingemann RO, Van Noorden CJ, Diekman MJ, et al. VEGF levels in plasma in relation to platelet activation, glycemic control, and microvascular complications in type 1 diabetes. *Diabetes Care*. 2013;36:1629-1634.
24. Kuryliszyn-Moskal A, Zarzycki W, Dubicki A, et al. Clinical usefulness of videocapillaroscopy and selected endothelial cell activation markers in people with Type 1 diabetes mellitus complicated by microangiopathy. *Adv Med Sci*. 2017;62:368-373.
25. Verma N, Liu M, Ly H, et al. Diabetic microcirculatory disturbances and pathologic erythropoiesis are provoked by deposition of amyloid-forming amylin in red blood cells and capillaries. *Kidney Int*. 2020;97:143-155.
26. Feng W, Liu S, Zhang C, et al. Comparison of cerebral and cutaneous microvascular dysfunction with the development of type 1 diabetes. *Theranostics*. 2019;9:5854-5868.
27. Liu W, Wang S, Soetikno B, et al. Increased retinal oxygen metabolism precedes microvascular alterations in type 1 diabetic mice. *Invest Ophthalmol Vis Sci*. 2017;58:981-989.
28. Kim JJ, Lee E, Ryu GR, et al. Hypoxia increases beta-cell death by activating pancreatic stellate cells within the islet. *Diabetes Metab J*. 2020;44:e22.
29. Bluestone JA, Herold K, Eisenbarth G. Genetics, pathogenesis and clinical interventions in type 1 diabetes. *Nature*. 2010;464:1293-1300.
30. Han J, Oh J, Ihm SH, et al. Peptide micelle-mediated curcumin delivery for protection of islet beta-cells under hypoxia. *J Drug Target*. 2016;24:618-623.
31. Moon RJ, Bascombe LA, Holt RI. The addition of metformin in type 1 diabetes improves insulin sensitivity, diabetic control, body composition and patient well-being. *Diabetes Obes Metab*. 2007;9:143-145.
32. Wang B, Zhang X, Liu M, et al. Insulin protects against type 1 diabetes mellitus-induced ultrastructural abnormalities of pancreatic islet microcirculation. *Microscopy (Oxf)*. 2020;69:381-390.
33. Nase GP, Tuttle J, Bohlen HG. Reduced perivascular PO2 increases nitric oxide release from endothelial cells. *Am J Physiol Heart Circ Physiol*. 2003;285:H507-H515.
34. Chen K, Pittman RN, Popel AS. Nitric oxide in the vasculature: where does it come from and where does it go? *A quantitative perspective*. *Antioxid Redox Signal*. 2008;10:1185-1198.

SUPPORTING INFORMATION

Additional supporting information may be found online in the Supporting Information section.